ADVANCING EARTH AND SPACE SCIENCES

AGU Advances

RESEARCH ARTICLE
10.1029/2026AV002516

Extreme Dry and Humid Heat Seasons Are Changing Asymmetrically

Catherine C. Ivanovich[1,2], Benjamin Cook[1,3], and Sonali McDermid[1,4]

[1]NASA Goddard Institute for Space Studies, New York, NY, USA, [2]NASA Postdoctoral Program Fellow, Oak Ridge Associated Universities, NASA NPP Program, Oak Ridge, TN, USA, [3]Division of Ocean Climate Physics, Lamont-Doherty Earth Observatory, Palisades, NY, USA, [4]Department of Environmental Studies, New York University, New York, NY, USA

Peer Review The peer review history for this article is available as a PDF in the Supporting Information.

Key Points:

- Extreme dry and humid heat events show distinct seasonality often not aligned with meteorological summer, even in the tropics
- Extreme heat seasons have expanded since the 1980s over about half of global land area, and this expansion is primarily asymmetric
- For most areas, observed changes in extreme heat during shoulder seasons cannot be explained by an intensification of baseline seasonality

Supporting Information:

Supporting Information may be found in the online version of this article.

Correspondence to:

C. C. Ivanovich,
cci2107@columbia.edu

Citation:

Ivanovich, C. C., Cook, B., & McDermid, S. (2026). Extreme dry and humid heat seasons are changing asymmetrically. *AGU Advances*, *7*, e2026AV002516. https://doi.org/10.1029/2026AV002516

Received 17 APR 2026
Accepted 16 AUG 2026

Author Contributions:

Conceptualization: Catherine C. Ivanovich, Benjamin Cook, Sonali McDermid
Data curation: Catherine C. Ivanovich
Formal analysis: Catherine C. Ivanovich
Funding acquisition: Catherine C. Ivanovich, Benjamin Cook, Sonali McDermid
Methodology: Catherine C. Ivanovich, Benjamin Cook, Sonali McDermid

Abstract Climate change is increasing the frequency of extreme heat events, including outside of the expected heat season. Unusually early or late extremes can create outsized impacts as individuals may be less acclimated to intense heat or unprepared to employ cooling strategies. Here we characterize the global seasonality of extreme dry and humid heat and quantify how seasonality is changing over time. We define local baseline heat seasons as the 3 months with the highest fraction of extreme heat events during 1980–1989. This extreme heat season is distinct from meteorological summer for many regions and captures most observed extreme heat days, even in the tropics where the amplitude of temperature seasonality is low. Over the last 45 years, extreme dry and humid heat seasons have significantly expanded over 50% and 48% of the global land area, respectfully, and this expansion is primarily asymmetric. Regions including the western United States, eastern China, northern Africa, and eastern Europe experienced a greater increase in the fraction of extreme dry and humid heat events following the historical extreme heat season, while regions that experienced a larger increase in the fraction of extremes preceding the extreme heat season include western Europe, southern Africa, and northwestern India. These observed asymmetrical changes in extreme heat occurrence in the shoulder seasons are generally not explainable by an intensification of preexisting seasonality driven by annual mean warming. These results highlight the need for extended heat alert systems and prompt further study of compound events where extreme heat seasons are increasingly overlapping with wildfire and hurricane seasons.

Plain Language Summary Extreme heat events can be more dangerous when they occur at unexpected times of year. However, we do not yet fully understand how the timing of heat extremes during the calendar year is changing. To address this challenge, we develop a definition of extreme heat seasonality distinct from other seasonal metrics and evaluate how these seasons have shifted over the past 45 years. We find that extreme dry and humid heat seasons have expanded over roughly half of the world and that this expansion has been asymmetric, with most regions experiencing greater increases in extreme heat frequency in the months after (western United States, eastern China, northern Africa, and eastern Europe) or before (western Europe, southern Africa, and northwestern India) the traditional extreme heat season. While we might expect that rising temperatures associated with climate change will make it easier for extreme heat events to occur during months that have historically been warmer on average, we find that this is insufficient to explain the observed changes in extreme heat seasonality. Understanding when in the calendar year extreme heat events are becoming more frequent is essential to managing risk, especially if extreme heat increasingly occurs alongside other seasonal climate hazards.

1. Introduction

Extreme heat can create outsized impacts when it occurs during unexpected times of year. When extreme heat takes place before the typical heat season, individuals may not have acclimated to higher temperatures or prepared adaptation strategies, such as installing air conditioning units or locating cooling centers (Anderson & Bell, 2010; Hajat et al., 2002; Lee et al., 2014). In contrast, extreme heat that occurs after the primary heat season may result in an accumulated heat burden which is more physiologically strenuous if it temporally compounds with earlier heatwaves during the heat season (Baldwin et al., 2019). Heat extremes occurring at new times of year are also detrimental to ecosystem health and agricultural yields when intersecting with growing seasons (Parker et al., 2020) and can cause compounding impacts when they extend into periods dominated by other seasonal hazards, such as hurricanes and wildfires (Fan et al., 2023; Matthews et al., 2019).

Project administration: Benjamin Cook, Sonali McDermid
Supervision: Benjamin Cook, Sonali McDermid
Validation: Catherine C. Ivanovich
Visualization: Catherine C. Ivanovich
Writing – original draft: Catherine C. Ivanovich
Writing – review & editing: Catherine C. Ivanovich, Benjamin Cook, Sonali McDermid

Extreme heat exceptional in its seasonality has reoccurred recently in Phoenix, AZ. In 2024, the city experienced an unprecedented 113 consecutive days above 100°F during the summer season, followed by 21 days in a row of all-time high temperatures in the month of October (Chow, 2024; Freedman, 2024; Figure S1 in Supporting Information S1). While daily maximum temperatures above 100°F are not unusual for Phoenix in terms of absolute magnitude, the duration of these high temperatures and their extension into the fall was record-breaking. Heat monitoring and cooling center operations were extended in response to the unusual fall temperatures (Gonzalez, 2024), demonstrating the increased management costs of a prolonged heat season. Further, the expansion of the 2024 extreme heat season is reflected in the seasonal distribution of heat-related mortality in the surrounding Maricopa County. As reported by the Department of Public Health, only 46% of the 608 reported heat-related deaths in 2024 occurred in July (the hottest month of the calendar year) in comparison to 64% in 2023 (Rubio et al., 2025). More recently, a regional and persistent heatwave in March 2026 shattered records in Phoenix and much of the western United States (Davis-Young, 2026; Erdman, 2026). In Las Vegas, the record breaking average March 2026 temperatures were also hotter than the previous record for the month of April. Nine days reached over 100°F in Phoenix during this heatwave, which had only happened once previously during the month of March in the historical record.

In addition to timing, whether extreme heat is simultaneously dry or humid also constrains its impacts. Dry heat tends to be more detrimental for plant and ecosystem health (Schauberger et al., 2017; Ting et al., 2023), while humid heat more strongly influences human health due to its limitation on the efficiency of sweat-based cooling (Mora et al., 2017; Parsons, 2006). Differentiating between these two types of heat is essential because they require different adaptation strategies for reducing heat exposure (Matthews et al., 2025) and because their timing and seasonality are often distinct (Ivanovich et al., 2024, 2026; Raymond et al., 2020; Rogers et al., 2021). Identifying how the timing of dry versus humid heat events are changing is thus essential for developing targeted adaptation strategies and management plans.

With ongoing anthropogenic climate change, extreme heat around the globe is increasing in frequency, intensity, and duration (Domeisen et al., 2022), but changes in the timing and seasonality of extreme heat are less well understood. Previous literature has shown that mean temperature seasonality is shifting in some regions of the globe. The warm season is lengthening across the Northern and Southern Hemisphere midlatitudes, and this extension of the warm season is expected to continue with future climate change (Christidis et al., 2007; Lin & Wang, 2022; Park et al., 2018; Scott et al., 2026; Wang et al., 2021; Weller et al., 2020). However, studies disagree on the degree to which changes in the date of summer onset versus withdrawal contribute to this lengthening of the warm season due to differences in seasonal definitions (Scott et al., 2026). Further, these studies do not evaluate the seasonality of extreme heat events, which may not align with seasonal mean changes (Lewis & King, 2017). Many regional studies have explored the drivers of out-of-season extreme heat events in areas such as North America (Ennis & Milrad, 2024; Milrad et al., 2025; Schwarz et al., 2020), South America (Ivanovich et al., 2025; Marengo et al., 2025; Perkins-Kirkpatrick et al., 2024), Europe (Lemus-Canovas et al., 2024; Sulikowska & Wypych, 2021), West Africa (Sambou et al., 2021), South Asia (Sanap et al., 2025; Zachariah et al., 2023), and East Asia (Wu et al., 2023). Additionally, global changes in heatwave intensity, frequency, and duration have been decomposed into patterns for individual meteorological seasons (Orlowsky & Seneviratne, 2012). Together, the existing body of literature identifies the potential increasing risk for extreme heat events outside of the summer season, but does not characterize overall global extreme heat seasonality or how it is changing over time.

To address these gaps in the literature, we develop a novel method for quantitatively defining extreme dry and humid heat seasonality. We apply this definition to characterize the heat seasons for a 1980–1989 baseline period and determine whether this seasonality has changed over the past 45 years. We then evaluate whether these changes to local heat seasons can be explained by a simple intensification of baseline seasonality associated with local annual mean warming. These results provide evidence of emerging risk for extreme heat at new times of year around the globe, with direct implications for risk management.

2. Methods

2.1. Data Set and Variable Selection

The primary data set used for this analysis is the Modern-Era Retrospective analysis for Research and Applications, Version 2 (MERRA-2). Due to the global scale of the analysis and the need to identify daily scale extreme heat events, reanalysis is the ideal data set type due to its continuity between variables and its high temporal and spatial resolution. Further, MERRA-2 has been widely used to investigate extreme dry and humid heat events (e.g., Bekris et al., 2023; Engdaw et al., 2022; Raymond et al., 2024). From this data set, we retrieve hourly 2-m temperature, 2-m dew point temperature, surface pressure, 10-m eastward wind, 10-m northward wind, surface incoming shortwave flux, surface net downward shortwave flux, surface absorbed longwave radiation, and surface net downward longwave flux. Where applicable, these hourly time series are aggregated to daily mean and daily maximum values.

We select wet bulb globe temperature (WBGT) as our humid heat metric because it has been shown to better reflect humans' experience of heat stress compared to other humid heat metrics (Budd, 2008; Buzan et al., 2015). Its widespread use in heat stress monitoring in the United States for applications such as outdoor sports, occupational hazards, and military training further motivates its use in the present study (Binkley et al., 2002; "OSHA Technical Manual,", 2017). WBGT is expressed as,

$$\mathrm{WBGT} = 0.7T_w + 0.2T_g + 0.1T_a \tag{1}$$

where T_w is the natural wet bulb temperature, T_g is the globe thermometer temperature, and T_a is the dry bulb temperature. We calculate hourly WBGT using the *thermofeel* toolbox (Brimicombe et al., 2022) and aggregate to daily maximum values.

Because reanalysis products have unique biases, particularly in surface moisture variables (Hirschi et al., 2025), we validate the patterns identified in the main text using the European Center for Medium-Range Weather Forecasts (ECMWF) Reanalysis v5 (ERA5). Reproductions of all global seasonality plots using ERA5 are included in Figures S2–S4 in Supporting Information S1. We find that the overall interpretation of our results is robust to the reanalysis product selected.

2.2. Methodologies

2.2.1. Extreme Heat Seasons and Shoulder Seasons Definitions

We define extreme dry and humid seasonality separately using dry bulb temperature and WBGT as our base heat metrics, respectively. We define local extreme dry heat seasons by first identifying 95th percentile daily maximum dry bulb temperatures (T95) across the full calendar year in a baseline period from 1980 to 1989 (the earliest decade in the MERRA-2 data set). We then calculate the 3 months of the calendar year with the highest frequency of T95 events. If these 3 months are consecutive, they are defined as the extreme dry heat season, designed to match the length of meteorological summer. If these 3 months are nonconsecutive, we mask the associated grid cell out of the seasonal analysis. We then define the shoulder seasons as the "pre-season" and "post-season," referring to the 2 months before and after the locally-defined extreme heat season, respectively. In regions where there are four distinct seasons, the pre-season (post-season) is analogous to spring (fall). We select a 2-month shoulder season length in order to capture events occurring on the edge of the baseline extreme heat season, to which we find most of the expansion of heat seasons is constrained across most of the globe. We repeat these methods using 95th percentile daily maximum WBGT (WBGT95) to define the extreme humid heat season and the humid heat shoulder seasons.

We define extreme heat events using fixed thresholds during a set baseline period in order to evaluate how events of a magnitude we have historically viewed as extreme are expanding into new times of year. This is in contrast to using a moving or detrended threshold for our extreme event definition, which would instead explore how the most extreme events per year are distributed throughout the calendar year. These *most* extreme events defined using moving or detrended thresholds may be expected to be more tightly constrained to the peak heat season throughout the historical record. Additionally, to evaluate the influence of the percentile threshold we select, we perform a sensitivity test using a slightly lower 90th percentile threshold for temperature and WBGT, recreating Figures 2–4 of our analysis as Figures S5–S7 in Supporting Information S1. We find strong overall agreement in the patterns identified using 95th and 90th percentiles, though the overall seasonal spread of extreme heat events is larger using the looser 90th percentile threshold in both dry and humid heat. We choose to retain the 95th percentile threshold for our definition of extreme heat events in the main manuscript due to its better reflection of truly unusual conditions.

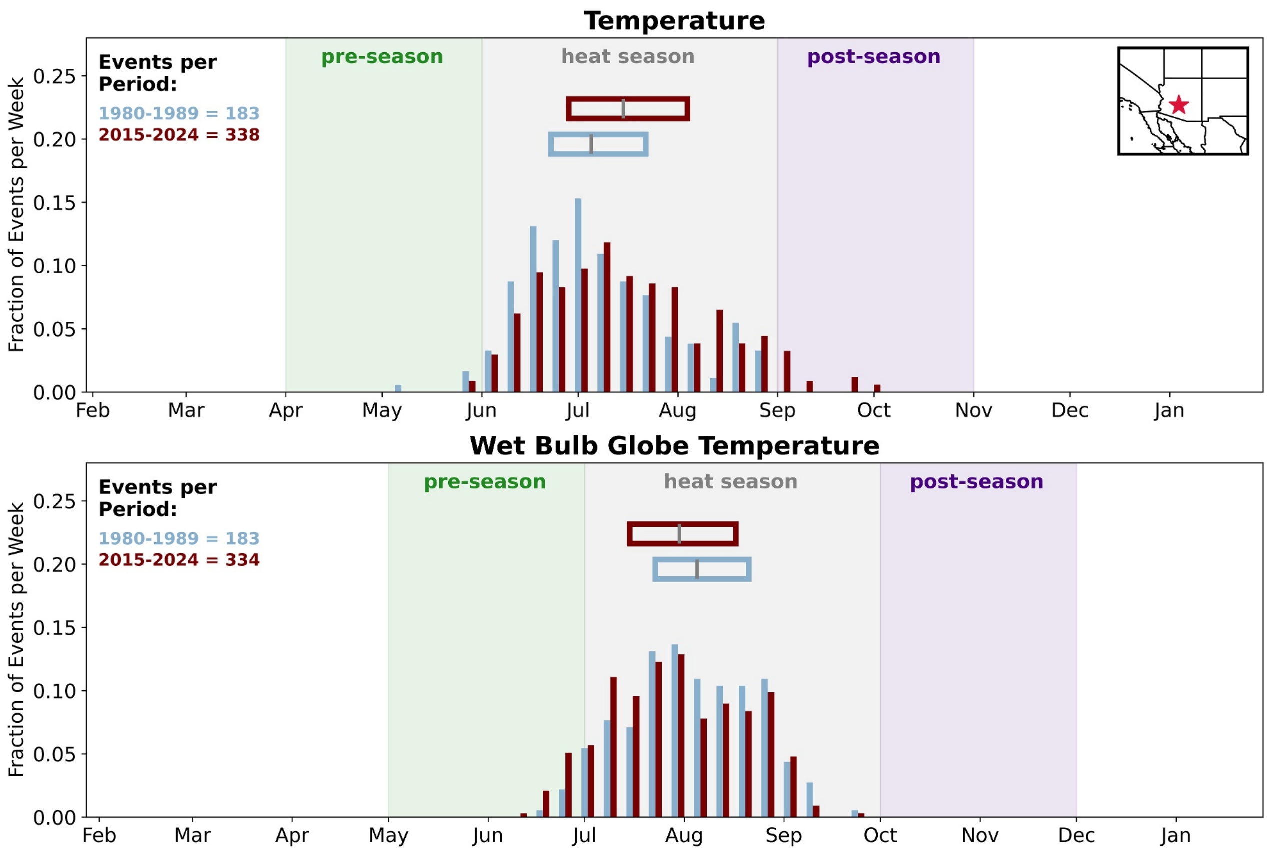

Figure 1. Seasonal distributions of T95 and WBGT95 events in early and late historical periods for Phoenix, AZ. Bars show the fraction of extreme events happening per week in the periods 1980–1989 (blue) and 2015–2024 (maroon). Box plots show the median and interquartile range for each period. The extreme heat season is defined as the 3 months per year with the highest fraction of extreme events in the baseline 1980–1989 period (gray). Pre-season (post-season) shown in green (purple) shading is defined as the 2 months before (after) the heat season.

2.2.2. Measuring Changes in Heat Seasonality

We measure changes in extreme heat seasonality by comparing the distribution of T95 and WBGT95 events in the baseline period (1980–1989, "early period") to the most recent decade in the historical record (2015–2024, "late period"). In each period and for both dry and humid heat, we sort extreme heat events into 52 bins for each week of the calendar year based on their date of occurrence. In order to account for the cyclic calendar year for locations whose heat season crosses the end of one year and start of the next, we shift the seasonal distribution by subtracting the week number with the highest frequency of extreme heat events in the historical record. If there is a tie between multiple weeks, we center the distribution on the middle week with peak frequency (rounding down in the case of even numbers). We then quantify measures of the center and spread of this seasonal distribution by computing the median and interquartile range (IQR) of the day of year of extreme heat events (repeated using mean and standard deviation in Figure S8 in Supporting Information S1). We also measure the asymmetry of observed changes in extreme heat seasonality based on the change in fraction of annual events occurring in the pre- versus post-seasons in the early and late periods.

The calculation of differences in the seasonal distribution of extreme heat events between two 10-year periods allows for a comparison of changes in conditions over the relatively short observational period of 45 years provided in the MERRA2 data set. However, interpretation of the changes observed between these two 10-year periods may be complicated by internal climate variability. We thus evaluate whether these patterns of change are robust against two additional calculation methods. We first perform a sensitivity test using 15-year periods, measuring changes between 1980–1994 and 2010–2024. We also calculate the linear trends from 1980 to 2024 in the counts of T95 and WBGT95 events during the pre- versus post-seasons. Our results are in broad agreement across these calculation methods, and the results of these additional analyses are presented in Figures S9–S11 and S17 in Supporting Information S1, respectively.

2.2.3. Asymmetry Explained by Baseline Seasonality Intensification

We test the degree to which observed changes in extreme heat seasonality are explained by an intensification of baseline seasonality. To do so, we calculate the annual mean temperature difference between the early and late periods at each grid cell:

$$\Delta T = T_{\text{mean}_{2015-2024}} - T_{\text{mean}_{1980-1989}} \quad (2)$$

We then add this temperature delta to all days in the baseline period, creating a synthetic time series which intensifies existing baseline extreme heat seasonality based on the annual mean warming at each global land grid cell. We then calculate the seasonal distribution of extreme heat events during this synthetic period and compare with that of the observed late period.

We first evaluate whether we can reject the null hypothesis that the seasonal distribution of extreme heat events across the full calendar year in the synthetic and observed late periods are pulled from the same distributions. We do so by performing a Kolmogorov–Smirnov (KS) Test between these two periods. For all grid cells whose KS-Test results in a p-value below 0.05, we accept that the observed distribution of extreme heat events throughout the full calendar year during the most recent 10 years of the historical record is significantly different from an intensification of baseline seasonality associated with local annual mean warming.

We then evaluate whether the observed changes in the fraction of extreme heat events occurring during the shoulder seasons are significantly different from what would be expected from an intensification of baseline seasonality. We calculate the post- versus pre-season asymmetry in the synthetic versus observed late historical period at each grid cell and compute the fraction of observed asymmetrical changes in extreme heat seasonality which are explained by this intensification of existing baseline seasonality. Testing whether these changes in shoulder season asymmetry are significant is complicated by the small sample size of events. For example, about 60% of land grid cells experienced zero extreme dry and humid events in the baseline period during at least one of the shoulder seasons. In order to evaluate significance while balancing these limitations to sample size, we perform a bootstrapping test. At each grid cell, we group all 10-years of data from the synthetic time series and calculate a probability density function (PDF) of the seasonal distribution of extreme heat events throughout the calendar year. This PDF is then used to define a cumulative density function (CDF) of the fraction of extreme heat events that have occurred by each day of the year. We then randomly resample with replacement from this CDF 5,000 times to generate another realization of the synthetic distribution's PDF. We repeat this resampling 1,000 times to generate a set of 1,000 PDFs from which we calculate the difference in the number of extreme heat events occurring in the post- versus pre-seasons, representing shoulder season extreme event asymmetry. We finally calculate the 5th and 95th percentiles in this measure of asymmetry and evaluate whether the observed asymmetry in the late period from 2015 to 2024 is outside of these confidence intervals. If so, we determine that the observed distribution of extreme events in the shoulder seasons cannot be explained by a simple intensification of baseline seasonality alone. We additionally perform a sensitivity test evaluating the impact of the number of times the CDF is resampled (between 500 and 10,000) and the number of PDFs generated (between 100 and 2,000), and we find that the sample size for both of these selections are sufficient for the present evaluation of significance, as the distributions do not change meaningfully at larger sample sizes. Example sensitivity test results are shown for grid cells with significant and insignificant differences in Figure S12 and S13 in Supporting Information S1.

We note that this analysis does not directly attribute changes in extreme heat seasonality to climate change. In addition to increasing annual mean temperature and WBGT, anthropogenic climate change can result in a wide variety of local dynamic and thermodynamic changes which differentially affect seasonal warming rates, variability, and persistence. In this analysis, we isolate the influence of annual mean warming on the intensification of existing temperature and WBGT seasonality and quantify any resulting asymmetrical changes to these seasonal distributions.

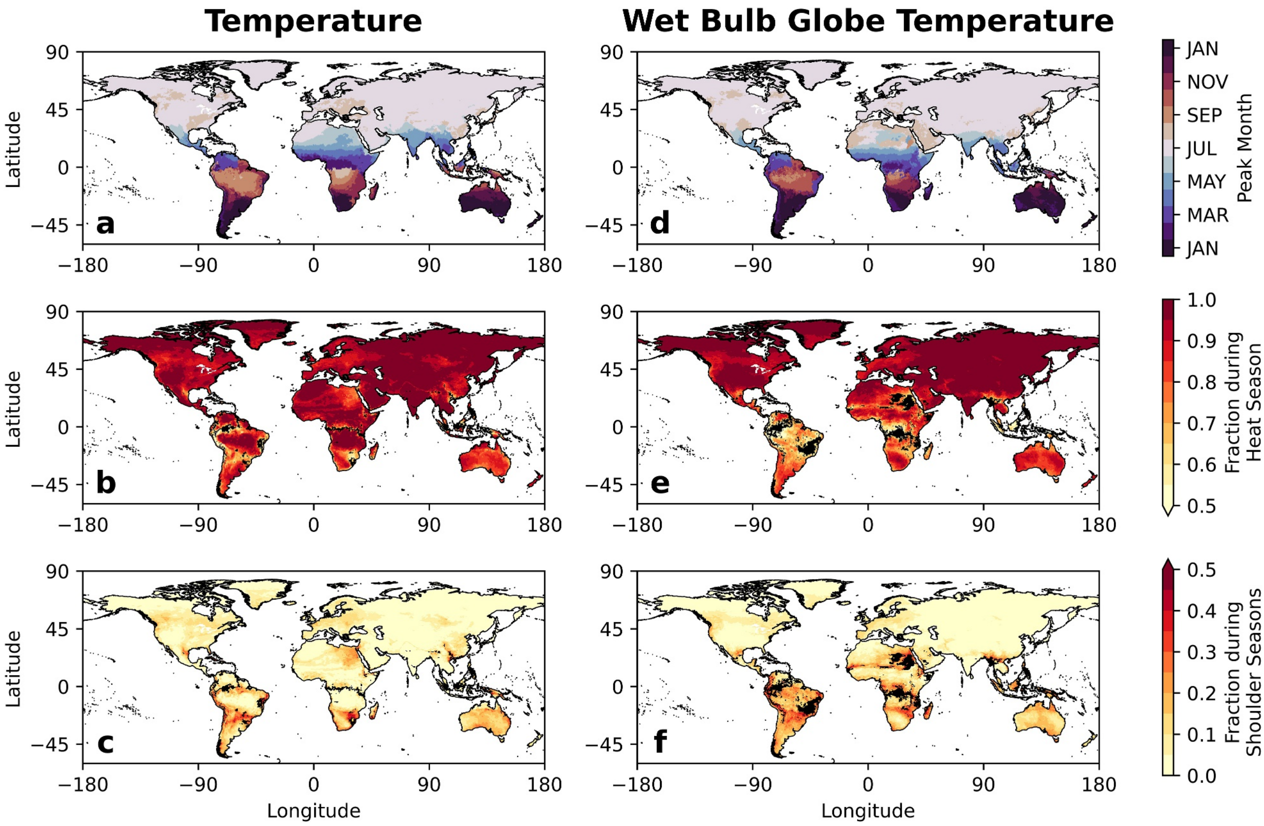

Figure 2. Global climatological extreme heat seasonality during the baseline period, 1980–1989. (a) Month with peak frequency of T95 events. Fraction of 1980–1989 T95 events happening during the locally defined (b) extreme dry heat season and (c) dry heat shoulder seasons. (d–f) Same as (a–c), but for WBGT95 events. The second and third rows have different colorbar ranges in order to better visualize spatial heterogeneity in each measurement. Black shading indicates grid cells without a consecutive 3-month heat season.

3. Results

3.1. What Is the Historical Seasonality of Extreme Heat and How Has It Changed?

As an example visualization of our approach to analysis and interpretation, we plot our results first for the grid cell closest to Phoenix, Arizona (Figure 1). We also include a mirrored example for a humid, tropical city—Phnom Penh, Cambodia—for comparison in Figure S14 in Supporting Information S1. In Phoenix, the baseline (1980–1989) dry heat season begins in June (Figure 1a, blue bars), while the humid heat season begins a month later in July (Figure 1b, blue bars), in agreement with previous literature using alternative seasonal definitions (Ivanovich et al., 2026). During this baseline period, T95 and WBGT95 events are concentrated within their respective heat seasons (99% of T95 events and 98% of WBGT95 events), with the highest frequency of both dry and humid heat extremes occurring in July. Zero extreme dry or humid heat events occur in the post-season during the baseline period, while two T95 events occur in the dry heat pre-season and three WBGT95 events occur in the humid heat pre-season.

Having identified well-constrained baseline extreme dry and humid heat seasons, we next evaluate whether this seasonality has changed over the historical period. We plot the distribution of T95 and WBGT95 events throughout the calendar year during the most recent 10 years in the historical record (maroon bars), from 2015 to 2024, alongside those of the baseline period and measure the change in the overall seasonal distribution of extremes. In Phoenix, the median date of dry heat extremes shifts significantly later by 10 days, while the median date of humid heat extremes shifts significantly earlier by 5.5 days (gray vertical lines in box plots; significance measured using a two-sided Wilcoxon Rank Sum Test). Further, the IQR of dry heat extreme dates increases by 7.5 days, while the change in spread of humid heat extremes is 4 days (edges of blue vs. maroon box plots), but these changes are both statistically insignificant (as measured using a two-sided Ansari-Bradley Test). We isolate

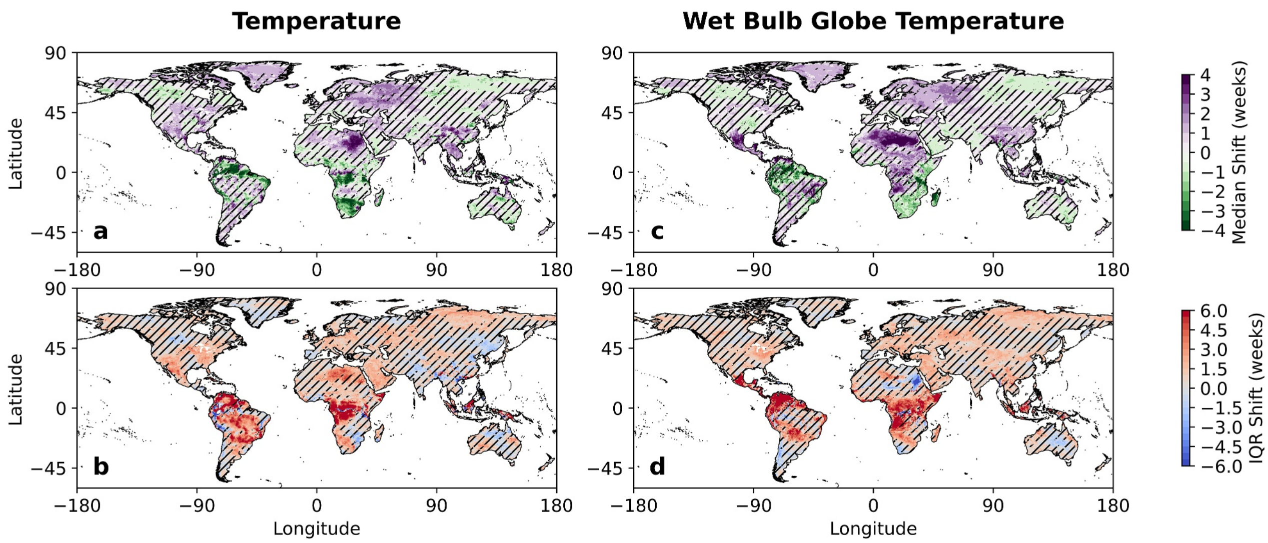

Figure 3. Change in the median and interquartile range of the day of year of extreme heat events from the early to late historical periods. Statistical significance for shifts in median (IQR) measured by a two-sided Wilcoxon Rank Sum (two-sided Ansari-Bradley) test at a p-value <0.05.

the asymmetric changes in shoulder season extremes by calculating the change in the fraction of annual extreme events which take place in the pre- and post-seasons between the early and late periods. We find that in Phoenix, the percent of annual T95 events taking place in the pre-season decreases from 2% to 1%, while the percent of events in the post-season increases from 0% to 6%. The share of WBGT95 events occurring in the pre-season increases from 3% to 7% over the historical period, while no WBGT95 events happen in the post-season in either time period. Together, these patterns indicate that in Phoenix, the dry heat season is expanding in length asymmetrically through an extension into the post-season. We note that this is in contrast to previous literature which has demonstrated that seasonal mean shifts in temperature are moving earlier in the calendar year or expanding symmetrically (Christidis et al., 2007; Lin & Wang, 2022; Park et al., 2018; Scott et al., 2026; Wang et al., 2021; Weller et al., 2020). However, the humid heat season in Phoenix is shifting earlier into the pre-season, but is not lengthening.

Applying our flexible definition for heat seasons across the globe captures the spatial diversity in the peak of extreme dry and humid heat seasonality (Figures 2a and 2d). This method expands upon traditional definitions of seasonality used for contextualizing extreme heat such as meteorological summer or the local three hottest months of the year. While the peak extreme dry and humid heat seasons are similar around the world, they are offset by 1 month throughout much of the tropics and subtropics including the Arabian Peninsula, northwestern Mexico, central India, and central Brazil—locations which are influenced by regional monsoon circulation.

Notably, extreme heat seasonality is well-defined, even throughout much of the tropics where there is relatively low overall seasonal temperature variability (Figures 2b and 2e). This is especially true for dry heat seasonality, while humid heat extremes spread more throughout the calendar year. Over 93% (86%) of the world's land area experiences over 80% of T95 (WBGT95) events during the local baseline extreme dry (humid) heat season. Most events occurring outside of the heat season occur during the shoulder seasons. About 94% (85%) of land grid cells experience more than 95% of T95 (WBGT95) events during the heat and shoulder seasons together (Figure S15 in Supporting Information S1). The shoulder seasons experience the largest fraction of extreme events in the Southern Hemisphere tropics and subtropics (Figures 2c and 2f). In the latitude band between 15 and 30°S, the average fraction of T95 (WBGT95) events which occur in the shoulder seasons is 17% (19%), compared to only 4% (4%) in the rest of the global land grid cells. This hemispheric contrast may be due to the lower overall seasonal amplitude of temperature and WBGT in the Southern Hemisphere associated with its lower land mass relative to the Northern Hemisphere (Figure S16 in Supporting Information S1). A few locations do not experience a consecutive 3-month heat season, as indicated by the black shading in Figure 2. Regions without a consecutive 3-month dry heat season include equatorial Africa and parts of the Amazon. These regions also lack a consecutive 3-month humid heat season, in addition to eastern Brazil and northeastern Africa. The larger overall

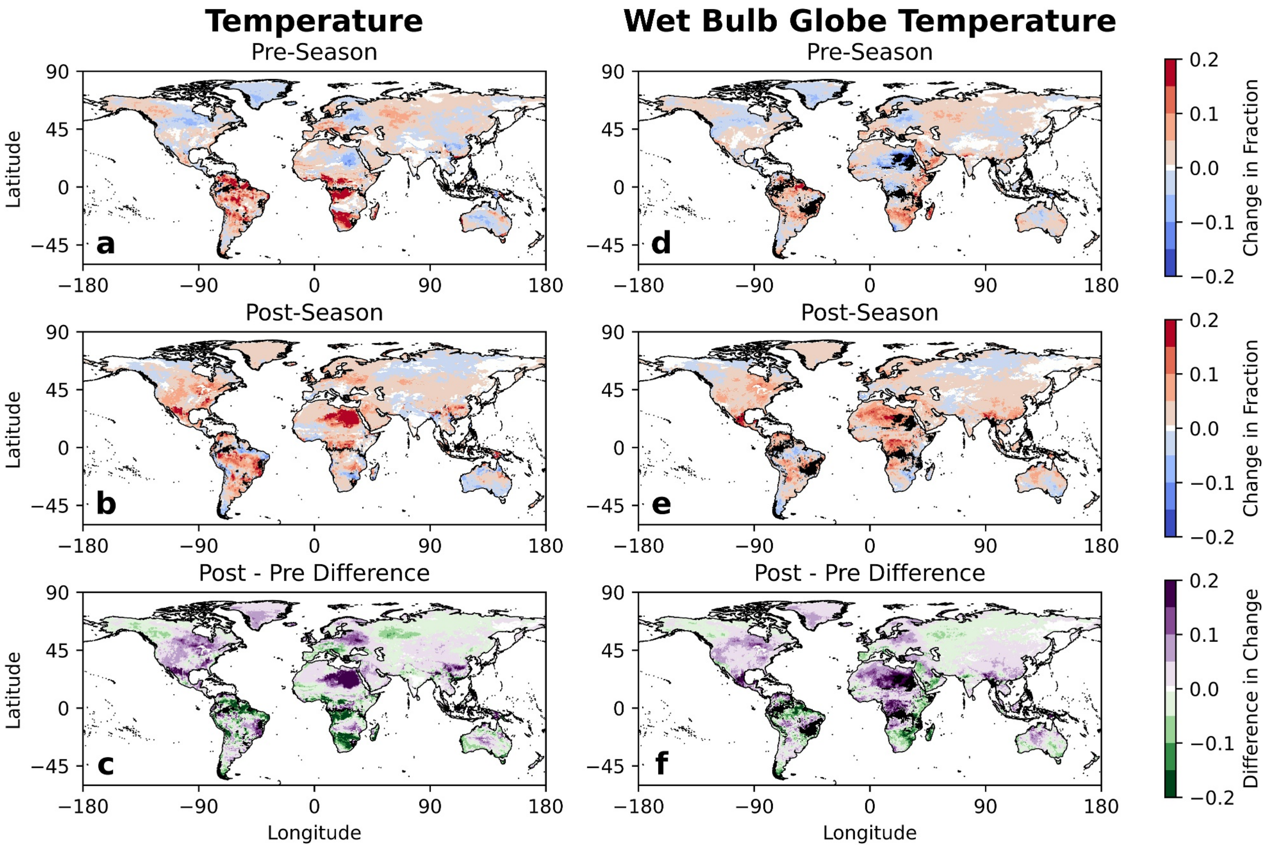

Figure 4. Change in the fraction of extreme heat events happening in the shoulder seasons. Top: Change in the fraction of annual events occurring in the pre-season from the early to late period. Middle: Change in the fraction of annual events occurring in the post-season from the early to late period. Bottom: Difference in the fractional change in shoulder season extreme heat events (post-season minus pre-season). Black shading indicates grid cells without a consecutive 3-month heat season.

seasonal variability of extreme humid heat reflects the joint influence of temperature and moisture fluctuations in driving humid heat extremes, as well as its lower seasonal amplitude relative to temperature around the globe (Figure S16 in Supporting Information S1). These overall patterns are in broad agreement between the MERRA2 and ERA5 data sets (Figure S2 in Supporting Information S1), although ERA5 exhibits slightly more seasonal spread in extreme dry and humid heat events throughout the calendar year.

We find asymmetric changes in the overall seasonal distribution of dry heat extremes in many regions throughout the globe (Figure 3). Statistically significant median shifts toward later dates in the calendar year occur throughout the southwestern and southeastern United States, northwestern Mexico, eastern Europe, northwestern Africa, and Southeast Asia. The median date of dry heat extremes shifts significantly earlier in equatorial Africa, South Africa, Pakistan, northern South America, and Eastern Australia. These median shifts are accompanied primarily by significant increases in the spread of the dry heat season as measured by increasing IQR, except in Pakistan where IQR is decreasing. The spread of extreme dry heat events is also increasing in the Arabian Peninsula, central Europe, and the United States Midwest, but there is limited significant asymmetry in these changes.

There are some distinctions between patterns observed for the dry and humid heat seasons. Significant shifts in the median extreme humid heat dates toward later dates occur over a larger spatial area throughout central Mexico and northern and central Africa relative to that of the dry heat season. Further, the median extreme humid heat date shifts earlier in the year over the United States Gulf Coast, southern and eastern Africa, and the southern Arabian Peninsula to a stronger degree than extreme dry heat events. Many regions experience extension of both the dry and humid heat seasons as measured by increasing IQR, but there are larger significant changes for humid heat seasons over the Maritime Continent and southern Mexico, while these expanded seasons are less significant in the western United States and the southern Arabian Peninsula relative to the dry heat season. These distinctions

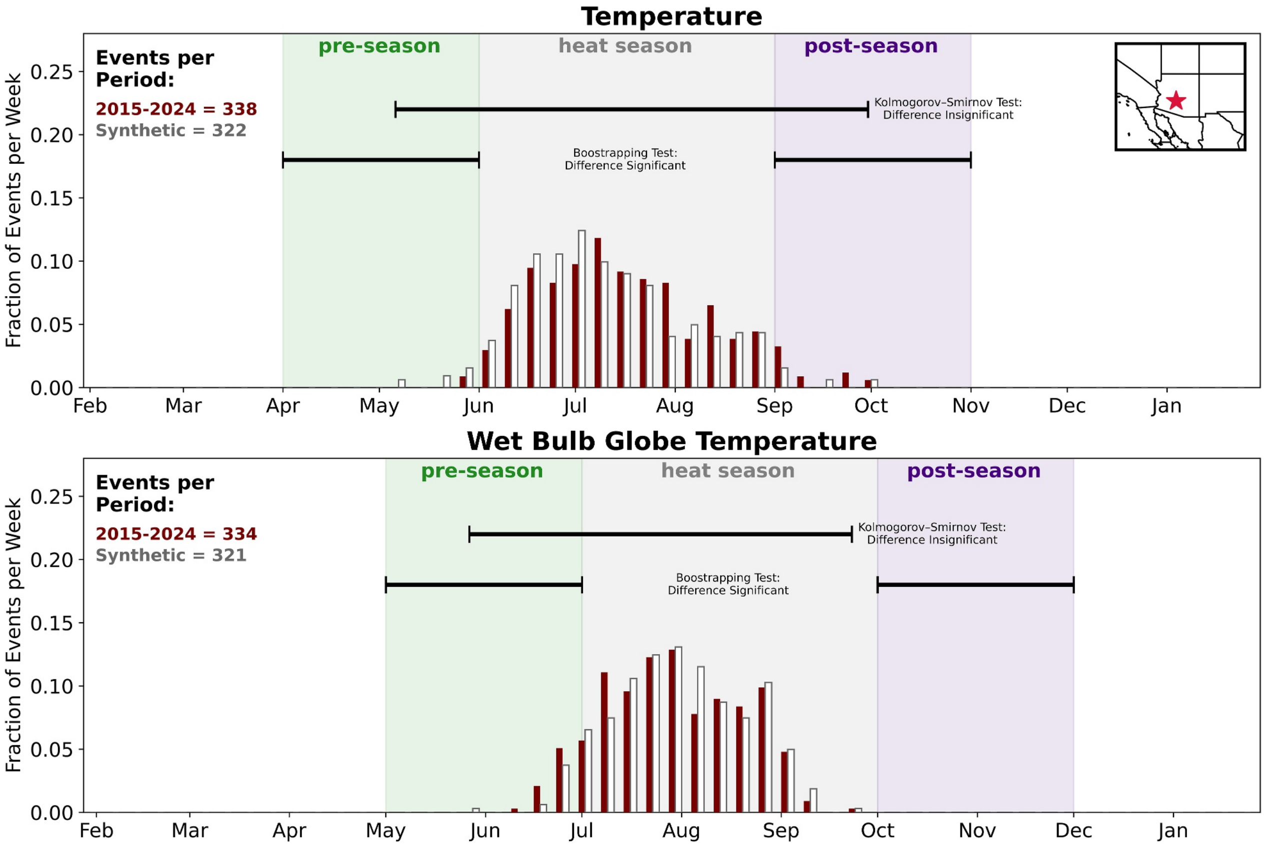

Figure 5. Seasonal distribution of extreme events in synthetic time series versus observed 2015–2024 period for Phoenix, AZ. Brackets highlight the data range tested by each significance test: KS-Test measures significance over full distribution; bootstrapping test measures significance over shoulder seasons.

between the changes in dry and humid heat seasonality demonstrate that seasonal changes in these two extreme heat types are not always in sync due to their distinct drivers. The observed directions of change for dry and humid heat seasons are broadly in agreement between regions with statistically significant changes between MERRA2 and ERA5 (Figure S3 in Supporting Information S1). Equatorial Africa is one region where the data sets disagree, exhibiting significantly larger shifts in the median date of humid heat extremes toward the post-season (pre-season) in MERRA2 (ERA5).

The share of extreme dry heat events occurring during the shoulder seasons is also changing asymmetrically throughout much of the globe, though the causes of this asymmetry vary by region (Figure 4, left column). For example, in regions such as the southeastern United States, the fraction of annual extreme events occurring in the post-season increases more strongly than in the pre-season. However, in regions such as northeastern Africa and eastern China, increases in the fraction of extremes occurring in the post-season coincide with decreases in the share of extremes during the pre-season. Southern and equatorial Africa experience expansion in both pre- and post-season extreme heat, with a larger increase in the share of pre-season extremes. In contrast, western Europe and northern Brazil experience decreases in the fraction of extreme dry heat events occurring in the post-season, contributing to the observed pre-season leaning asymmetry. Many of these regions also experience asymmetrical changes in the fraction of extreme humid heat events occurring during the shoulder seasons, though not always with the same asymmetry as the dry heat seasons (Figure 4, right column). This includes the Arabian Peninsula, which experiences a larger increase in the fraction of humid heat extremes occurring in the pre-season than post-season; and equatorial Africa, which experiences a decrease in the fraction of extremes occurring in the pre-season and an increase in the post-season. The overall direction of shoulder season asymmetry is largely in agreement with the difference in linear trends in the annual counts of T95 and WBGT95 events occurring in the post- versus pre-seasons, shown in Figure S17 in Supporting Information S1. Patterns identified using MERRA2 and ERA5 are again in strong agreement throughout most of the globe (Figure S4 in Supporting Information S1).

A few areas of disagreement include central Argentina and equatorial Africa for dry heat extremes, and northwestern South America and equatorial Africa for humid heat extremes. The repeated disagreement between these reanalysis products in equatorial Africa has been previously highlighted (Engdaw et al., 2022), identifying regional biases in MERRA2 extreme heat event identification.

3.2. Are These Changes Explained by an Intensification of Baseline Seasonality?

Changes in the share of extreme heat events taking place in the heat season versus shoulder seasons could be explained by a simple intensification of local baseline seasonality due to secular warming trends. For example, dry bulb temperatures in Phoenix on average are higher in September (1 month after the local dry heat season demise) than they are in May (1 month before the local dry heat season onset). This suggests that a simple shifting up of the annual average temperature will make it easier to cross the T95 threshold in the post-season than the pre-season, resulting in an asymmetric change in the fraction of extreme heat events taking place in each shoulder season. We test whether this intensification of local baseline seasonality can explain the observed global changes to heat seasonality as described by our synthetic time series over the historical period using the method described in Section 2.2.3 and visualized for Phoenix in Figure S18 in Supporting Information S1. This intensification of existing dry (humid) heat seasonality results in an increase of 124 (127) extreme heat events during the heat season, 5 (10) extreme heat events during the pre-season, and 9 (0) extreme heat events during the post-season in Phoenix.

We then compare the distribution of extreme heat events throughout the calendar year in the synthetic distribution (white bars, Figure 5) with the observed late period (maroon bars, Figure 5). In Phoenix, we find that the full seasonal distributions of dry and humid heat for 2015–2024 are not significantly different from distributions from our null warming case (two-sided Kolmogorov-Smirnov test; $p \approx 1$ for both the dry and humid heat distributions). This indicates that changes in the overall seasonality of both dry and humid heat, dominated by changes in the bulk of the distributions during their respective heat seasons, cannot be distinguished from changes associated with the intensification of baseline seasonality resulting from background warming trends. However, observed asymmetrical changes in the fraction of extreme heat events occurring in the shoulder seasons are significantly different from those of the synthetic period for the extreme dry and humid heat seasons. For example, the 5th and 95th percentiles of the difference between the fraction of T95 events occurring in the post- and pre-season generated by this resampling of the synthetic distribution are −0.009 and 0.003, respectively. The observed difference during the last 10 years of the historical record in Phoenix of 0.05 is much greater than the 95th percentile of the synthetic realizations, indicating that the expansion of the extreme dry heat season into the post-season cannot be explained by Phoenix's baseline temperature seasonality being intensified through annual mean warming alone. Similarly, the observed difference between the fraction of WBGT95 extremes occurring in the post- versus pre-season (−0.07) in the 2015–2024 period is lower than the fifth percentile of the synthetic realizations (−0.05), meaning the shift of the extreme humid heat season into the pre-season also cannot be explained solely by an intensification of baseline humid heat seasonality.

Globally, changes in the overall distribution of extreme heat events throughout the full calendar year are predominantly explainable by intensification of existing heat seasonality due to local annual mean warming. Only 14% of land grid cells experience a change in their overall extreme dry heat season which is significantly different from that of their associated synthetic distribution, in regions including the southeastern United States, the Amazon, and central and eastern Africa. Similarly, only 16% of land grid cells have experienced shifts in the overall seasonal distribution of extreme humid heat significantly different from an intensified baseline seasonality in regions including the southeastern United States, northeastern Africa, northwestern India, and eastern China. These significant changes occur in regions which experience shifts in the same direction both within the heat season and into the shoulder seasons (Figures 3 and 4, Figure S19 in Supporting Information S1). For example, extreme humid heat in eastern China experiences a shift in the median date of occurrence, an asymmetrical change in the first and last months of the heat season, and an asymmetrical change in the shoulder seasons which all shift toward later dates in the calendar year.

In contrast, intensification of baseline extreme heat seasonality cannot explain most observed changes in extreme heat occurrences in the shoulder seasons around the world. The number of extreme dry and humid heat events in the pre- versus post-seasons are significantly different from that expected from an intensification of baseline seasonality associated with local annual mean warming in about 80% of land grid cells (Figures 6c and 6d, purple

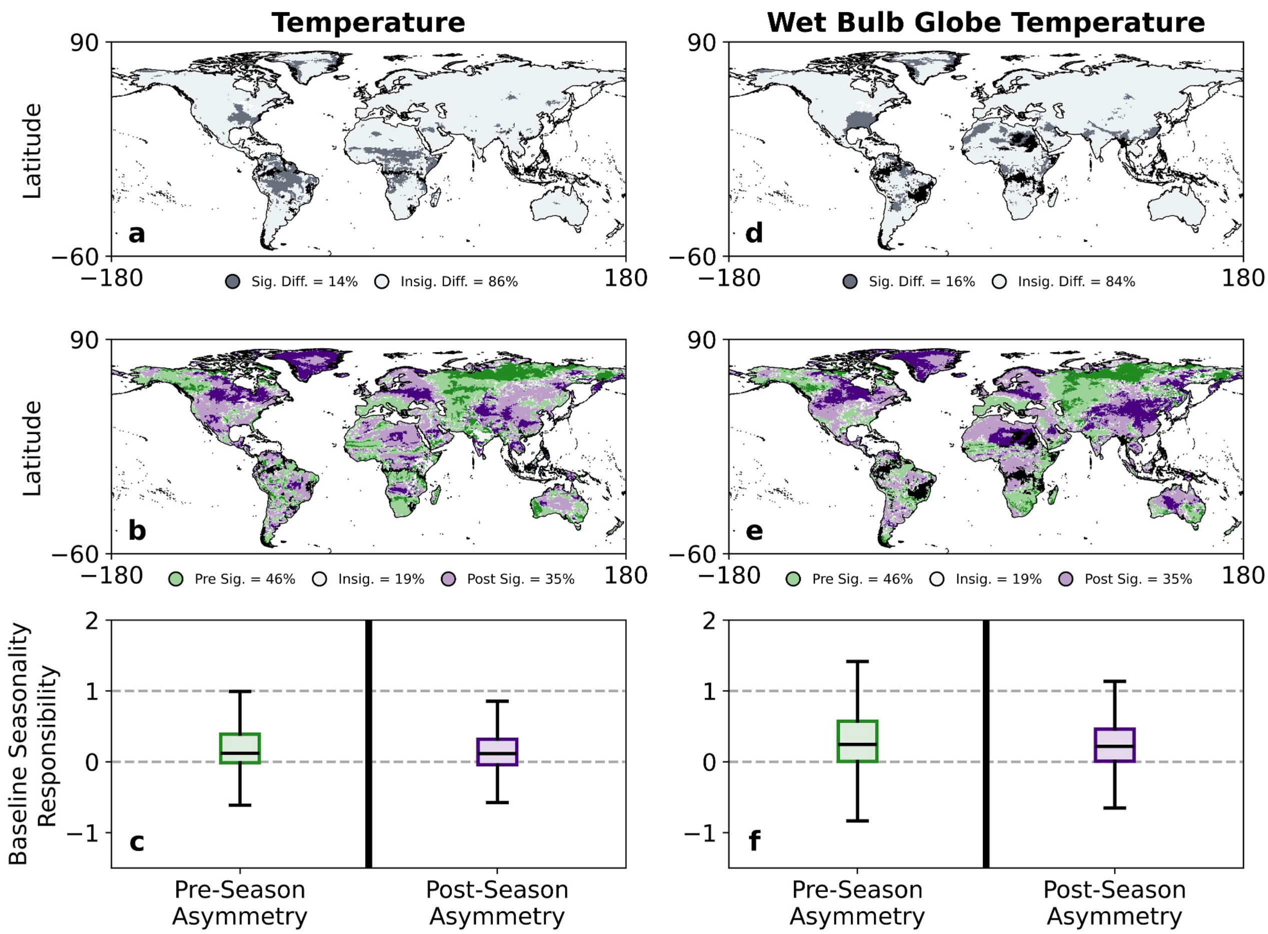

Figure 6. Evaluation of whether seasonal extreme heat frequency changes can be explained by an intensification of baseline seasonality. Locations across the globe where existing seasonality in the 1980s shifted up by annual mean warming does not explain observed changes in (top) overall extreme heat seasonality as measured by a Kolmogorov–Smirnov Test with a p-value below 0.05 and (middle) shoulder season asymmetry as measured by bootstrapping test. Green (purple) shades indicate that observed asymmetry is larger in the pre-season (post-season) than predicted by intensification of baseline seasonality. Darker shades of each color indicate that the observed asymmetry is in the opposite direction than in the synthetic distribution. Bottom: Box plots showing the share of asymmetry explained by intensifying existing extreme heat seasonality, categorized by whether that asymmetry favors pre- or post-season extremes. Only grid cells which exhibit at least a 5% shoulder season asymmetry as measured by Figures 4c and 4f are included.

and green grid cells). Further, about 99% of grid cells that have experienced asymmetrical changes in shoulder season extremes (where the observed asymmetry as shown in Figures 4c and 4f is greater than 5%) now experience extreme event distributions in the shoulder seasons which are significantly different from what would be expected from an intensification of existing seasonality (Figures 6c and 6f). Indeed, many regions which would be expected to experience larger increases in T95 events during the pre-season because of higher baseline temperatures in those months instead experience a greater increase in post-season T95 events (e.g., eastern Europe, the southwest United States, and northern Canada). The opposite is also true: western Australia and northern Russia experience greater expansion of the dry heat season into the pre-season while an intensification of baseline seasonality would have predicted a larger shift into the post-season. Similar patterns hold for the extreme humid heat season. Observed asymmetrical changes in the fraction of WBGT95 events occurring in the shoulder seasons act in the opposite direction to expectations from baseline seasonality in regions including the northwest United States, eastern Europe, eastern China, and northern Africa (baseline seasonality facilitates pre-season extremes; post-season asymmetry observed), northern Russia, and western Canada (baseline seasonality facilitates post-season extremes; pre-season asymmetry observed).

4. Discussion and Conclusion

We have demonstrated that, for most global land areas, dry and humid heat seasonality is well-defined and distinct from typical definitions of summer, even across low latitude regions where seasonal temperature variation is low. Further, we show that extreme heat seasonality has changed significantly over the past 45 years, with extreme dry and humid heat seasons expanding throughout much of the world and asymmetric changes in extreme heat occurrence during the shoulder seasons. An intensification of baseline seasonality due to local annual mean warming associated with anthropogenic climate change is insufficient to explain the observed asymmetric changes in the fraction of extreme heat events which now occur during the shoulder seasons. Instead, other regional processes are driving spatially heterogeneous increases in the fraction of extreme heat events occurring before and after the traditional dry and humid heat seasons.

Our results showcase how extreme heat seasonality is distinct from the warm season in many regions and that changes in the seasonality of extreme heat do not always align with changes in other conventional seasonal diagnostics. Several studies (Christidis et al., 2007; Lin & Wang, 2022; Park et al., 2018; Scott et al., 2026; Wang et al., 2021; Weller et al., 2020) have demonstrated that the warm season is lengthening throughout the midlatitudes, but disagree on whether this lengthening is symmetric. The seasonal definitions in these studies calculate summer onset using daily mean temperature records, smoothing them with a polynomial or Fourier series and calculating summer onset and withdrawal as the first and last day above a locally defined 75th percentile temperature threshold. Studies reporting asymmetric lengthening of Northern Hemisphere midlatitude summer find these changes are dominated by earlier onset dates (Park et al., 2018; Wang et al., 2021). We demonstrate in the present analysis that smoothed seasonal changes do not necessarily align with changes in the timing of individual extreme heat events. Changes to pre-season extreme events (analogous to spring in the midlatitudes) do dominate the asymmetrical changes in heat occurrence in regions including western Europe and northeastern Russia, but much of the United States, eastern Europe, and eastern China have experienced changes in shoulder season extreme heat frequency that are dominated by increases in fall extremes. Additionally, while previous studies indicate that the average warm season length is increasing significantly in the midlatitudes, our results show that this is not necessarily the case for the extreme heat season and regions including eastern Russia have even experienced contracting extreme heat seasons.

These differences are sensitive to metric choice and seasonal definitions, the appropriate selection of which depends on the impacts that are most relevant to researchers and stakeholders. Full seasonal changes as measured by warm season onset and withdrawal may be more relevant to impacts on growing seasons, snowpack and water availability, and drought which each operate over longer time periods (Evan & Eisenman, 2021; Körner et al., 2023; Van Loon et al., 2014). In contrast, individual extreme heat days or heatwaves may more strongly influence human and animal health, as the impacts of these hazards can manifest on much shorter timescales (Xu et al., 2016, 2018). The shifting of extreme heat event timing can also create cascading indirect impacts including limited potential to reduce electricity demand in schools during heatwaves which occur during the academic year rather than on summer breaks ("Sustainability," 2026) and increased demand for informal cooling strategies at new times of year such as public pool seasons (Howard, 2025). The present analysis' focus on individual extreme events also emphasizes that long term asymmetric changes in shoulder season extreme heat occurrence do not preclude individual heatwaves in other times of year. For example, while extreme heat frequency in the city of Rio de Janeiro is increasing more strongly in the fall, a record-breaking and deadly spring heatwave occurred in this city in 2023 (Collazo et al., 2025; Ivanovich et al., 2025; Marengo et al., 2025; Pampuch et al., 2025). This and similar case studies emphasize that isolated extreme events must be evaluated individually and that unseasonable extremes can still occur outside of new normals.

A limitation of this study is the small sample size in shoulder season extreme events. Extreme event statistics require careful evaluation due to the fact that extreme events are inherently rare. By investigating extreme heat events happening during months when they have historically been unusual or unprecedented, we further restrict the sample size for analysis. This limits the use of many traditional methods for evaluating statistical significance, which we address by developing a bootstrapping technique to increase the number of synthetic time series realizations. This approach is imperfect but provides a best estimate of statistical significance using only reanalysis data sets. In future analyses, these challenges could be addressed using global climate models by first evaluating whether the observed asymmetric changes in extreme heat seasonality are well-captured by models, and then leveraging large ensembles to directly evaluate the statistical significance of these changes. Such analyses could also evaluate whether observed changes in shoulder season extreme heat frequency are projected to continue in the future.

Regional analyses investigating the dynamics of the observed changes in extreme heat seasonality are beyond the scope of the present paper, but would help improve our understanding of the potential process drivers of the asymmetric and spatially heterogeneous changes we documented. Indeed, the local mechanisms generating increases in the frequency of extreme dry versus humid heat in the pre- and post-seasons are likely distinct. For example, the summer and fall of 2024 were unusually dry in Phoenix (Freedman, 2024), conditions that intensify extreme heat during the fall in this region (Ivanovich et al., 2026) and could have contributed to the record breaking heat along with longer-term drivers including anthropogenic climate change and El Niño (Jha et al., 2025). In contrast, the record-shattering March 2026 temperatures in Phoenix and the broader Southwest United States were associated with a particularly persistent high pressure system, though rapid attribution estimates that the recorded regional temperatures would have been virtually impossible without the influence of climate change (Clarke et al., 2026). These individual events motivate further investigations into how seasonal trends in circulation and surface moisture (as observed for the Southwest United States in Jacobson et al., 2024) may be driving distinct seasonal trends in extreme dry and humid heat frequency. The role of large scale modes of climate variability should also be assessed in the role of temporal variability of extreme heat seasonality, particularly as it complicates interpretation of long term trends. Other local drivers of extreme heat seasonality including changes to land cover and land use change should also be explored, given human action associated with irrigation and agricultural production can differ seasonally throughout the calendar year (Singh et al., 2018).

Future regional analyses should also explore the implications of changes in the seasonal distribution of extreme heat events for increasing risk of compound extremes. In the western United States, for example, extension of the extreme heat season into the fall increases the overlap in the extreme heat and wildfire seasons (Chen et al., 2024; Jones-Ngo et al., 2025), while in the southeastern United States, more rapid expansion of the extreme heat season into the fall increases overlap in the extreme heat and Atlantic hurricane seasons (Feng et al., 2022; Matthews et al., 2019). Because compound extremes cause socioeconomic impacts far greater than the sum of their parts (AghaKouchak et al., 2020; Zscheischler et al., 2018), understanding their potentially increasing risk is essential for disaster management and adaptation planning.

Conflict of Interest

The authors declare no conflicts of interest relevant to this study.

Availability Statement

The publicly available datasets used in this analysis are accessible via the following websites: MERRA2 (Gelaro et al., 2017), https://gmao.gsfc.nasa.gov/reanalysis/merra-2/data_access/; and ERA5 (Hersbach et al., 2020, 2023a, 2023b), https://cds.climate.copernicus.eu/datasets/reanalysis-era5-single-levels?tab=overview and https://cds.climate.copernicus.eu/datasets/reanalysis-era5-pressure-levels?tab=overview. All code for analysis and figure production is publicly available on Github at https://github.com/ccivanovich/Extreme_Heat_Seasonality and is preserved on Zenodo at https://doi.org/10.5281/zenodo.19582097 (Ivanovich, 2026). Figures were made with Matplotlib (Hunter, 2007) and Cartopy, available at https://doi.org/10.1109/MCSE.2007.55 and http://scitools.org.uk/cartopy, respectively. Analysis was completed using Xarray (Hoyer & Hamman, 2017) and SciPy (Virtanen et al., 2020), available at https://doi.org/10.5334/jors.148 and https://doi.org/10.1038/s41592-019-0686-2, respectively.

Acknowledgments
C. I. is supported by the NASA Postdoctoral Program (NPP) Fellowship. Research was sponsored by the National Aeronautics and Space Administration (NASA, ORAU-80HQTR21CA005) through a contract with ORAU. The views and conclusions contained in this document are those of the authors and should not be interpreted as representing the official policies, either expressed or implied, of the National Aeronautics and Space Administration (NASA) or the U.S. Government. The U.S. Government is authorized to reproduce and distribute reprints for Government purposes notwithstanding any copyright notation herein.

References

AghaKouchak, A., Chiang, F., Huning, L. S., Love, C. A., Mallakpour, I., Mazdiyasni, O., et al. (2020). Climate extremes and compound hazards in a warming world. *Annual Review of Earth and Planetary Sciences*, *48*(1), 519–548. https://doi.org/10.1146/annurev-earth-071719-055228

Anderson, G. B., & Bell, M. L. (2010). Heat waves in the United States: Mortality risk during heat waves and effect modification by heat wave characteristics in 43 U.S. communities. *Environmental Health Perspectives*, *119*(2), 210–218. https://doi.org/10.1289/ehp.1002313

Baldwin, J. W., Dessy, J. B., Vecchi, G. A., & Oppenheimer, M. (2019). Temporally compound heat wave events and global warming: An emerging hazard. *Earth's Future*, *7*(4), 411–427. https://doi.org/10.1029/2018EF000989

Bekris, Y., Loikith, P. C., & Neelin, J. D. (2023). Short warm distribution tails accelerate the increase of humid-heat extremes under global warming. *Geophysical Research Letters*, *50*(11), e2022GL102164. https://doi.org/10.1029/2022GL102164

Binkley, H. M., Beckett, J., Casa, D. J., Kleiner, D. M., & Plummer, P. E. (2002). National athletic trainers' association position statement: Exertional heat illnesses. *Journal of Athletic Training*, *37*(3), 329–343.

Brimicombe, C., Di Napoli, C., Quintino, T., Pappenberger, F., Cornforth, R., & Cloke, H. L. (2022). Thermofeel: A python thermal comfort indices library. *SoftwareX*, *18*, 101005. https://doi.org/10.1016/j.softx.2022.101005

Budd, G. M. (2008). Wet-bulb globe temperature (WBGT)—Its history and its limitations. *Journal of Science and Medicine in Sport*, *11*(1), 20–32. https://doi.org/10.1016/j.jsams.2007.07.003

Buzan, J. R., Oleson, K., & Huber, M. (2015). Implementation and comparison of a suite of heat stress metrics within the Community Land Model version 4.5. *Geoscientific Model Development*, *8*(2), 151–170. https://doi.org/10.5194/gmd-8-151-2015

Chen, C., Schwarz, L., Rosenthal, N., Marlier, M. E., & Benmarhnia, T. (2024). Exploring spatial heterogeneity in synergistic effects of compound climate hazards: Extreme heat and wildfire smoke on cardiorespiratory hospitalizations in California. *Science Advances*, *10*(5), eadj7264. https://doi.org/10.1126/sciadv.adj7264

Chow, D. (2024). *Phoenix ends 21-day streak of record October heat*. NBC News. Retrieved from https://www.nbcnews.com/science/climate-change/phoenix-fall-heat-wave-records-october-rcna175349

Christidis, N., Stott, P. A., Brown, S., Karoly, D. J., & Caesar, J. (2007). Human contribution to the lengthening of the growing season during 1950–99. *Journal of Climate*, *20*(21), 5441–5454. https://doi.org/10.1175/2007JCLI1568.1

Clarke, B., Keeping, T., Zachariah, M., Barnes, C., Mitra, S., Vahlberg, M., & Otto, F. (2026). Record-shattering March temperatures in Western North America virtually impossible without climate change. Retrieved from https://www.worldweatherattribution.org/record-shattering-march-temperatures-in-western-north-america-virtually-impossible-without-climate-change/

Collazo, S., Barriopedro, D., García-Herrera, R., & Beguería, S. (2025). Extreme heat and mortality in the state of Rio de Janeiro in November 2023: Attribution to climate change and ENSO. *Natural Hazards and Earth System Sciences*, *25*(9), 3221–3238. https://doi.org/10.5194/nhess-25-3221-2025

Davis-Young. (2026). Temperatures shattered records in Phoenix and across the west. *KJZZ*. Retrieved from https://www.kjzz.org/science/2026-04-01/march-temperatures-shattered-records-in-phoenix-and-across-the-west

Domeisen, D. I. V., Eltahir, E. A. B., Fischer, E. M., Knutti, R., Perkins-Kirkpatrick, S. E., Schär, C., et al. (2022). Prediction and projection of heatwaves. *Nature Reviews Earth & Environment*, *4*(1), 36–50. https://doi.org/10.1038/s43017-022-00371-z

Engdaw, M. M., Ballinger, A. P., Hegerl, G. C., & Steiner, A. K. (2022). Changes in temperature and heat waves over Africa using observational and reanalysis data sets. *International Journal of Climatology*, *42*(2), 1165–1180. https://doi.org/10.1002/joc.7295

Ennis, K. E., & Milrad, S. M. (2024). Man, it's a hot one: Trends and extremes in Florida autumn heat stress. *International Journal of Climatology*, *44*(5), 1816–1830. https://doi.org/10.1002/joc.8415

Erdman, J. (2026). Record warmest March in dozens of cities from California to Texas. Retrieved from https://weather.com/news/weather/news/2026-04-01-record-warmest-march-cities-west-rockies-plains

Evan, A., & Eisenman, I. (2021). A mechanism for regional variations in snowpack melt under rising temperature. *Nature Climate Change*, *11*(4), 326–330. https://doi.org/10.1038/s41558-021-00996-w

Fan, X., Miao, C., Zscheischler, J., Slater, L., Wu, Y., Chai, Y., & AghaKouchak, A. (2023). Escalating hot-dry extremes amplify compound fire weather risk. *Earth's Future*, *11*(11), e2023EF003976. https://doi.org/10.1029/2023EF003976

Feng, K., Ouyang, M., & Lin, N. (2022). Tropical cyclone-blackout-heatwave compound hazard resilience in a changing climate. *Nature Communications*, *13*(1), 4421. https://doi.org/10.1038/s41467-022-32018-4

Freedman, A. (2024). *Phoenix shatters extreme heat records into fall*. Axios. Retrieved from https://www.axios.com/2024/10/17/phoenix-shatters-heat-records-fall

Gelaro, R., McCarty, W., Suárez, M. J., Todling, R., Molod, A., Takacs, L., et al. (2017). The modern-era retrospective analysis for research and applications, version 2 (MERRA-2). *Journal of Climate*, *30*(14), 5419–5454. https://doi.org/10.1175/JCLI-D-16-0758.1

Gonzalez, J. R. (2024). Cooling centers to remain open in Phoenix through record-breaking heat. Retrieved from https://www.azcentral.com/story/news/local/phoenix-weather/2024/09/28/phoenix-will-keep-cooling-centers-open-through-oct-7/75415153007/

Hajat, S., Kovats, R. S., Atkinson, R. W., & Haines, A. (2002). Impact of hot temperatures on death in London: A time series approach. *Journal of Epidemiology & Community Health*, *56*(5), 321–372. https://doi.org/10.1136/jech.56.5.367

Hersbach, H., Bell, B., Berrisford, P., Biavati, G., Horányi, A., Muñoz Sabater, J., et al. (2023a). ERA5 hourly data on single levels from 1940 to present [Dataset]. *Copernicus Climate Change Service (C3S) Climate Data Store (CDS)*. https://doi.org/10.24381/cds.adbb2d47

Hersbach, H., Bell, B., Berrisford, P., Biavati, G., Horányi, A., Muñoz Sabater, J., et al. (2023b). ERA5 hourly data on pressure levels from 1940 to present [Dataset]. *Copernicus Climate Change Service (C3S) Climate Data Store (CDS)*. https://doi.org/10.24381/cds.bd0915c6

Hersbach, H., Bell, B., Berrisford, P., Hirahara, S., Horányi, A., Muñoz-Sabater, J., et al. (2020). The ERA5 global reanalysis. *Quarterly Journal of the Royal Meteorological Society*, *146*(730), 1999–2049. https://doi.org/10.1002/qj.3803

Hirschi, M., Stradiotti, P., Crezee, B., Dorigo, W., & Seneviratne, S. I. (2025). Potential of long-term satellite observations and reanalysis products for characterising soil drying: Trends and drought events. *Hydrology and Earth System Sciences*, *29*(2), 397–425. https://doi.org/10.5194/hess-29-397-2025

Howard, H. (2025). A heat wave hits New York earlier than usual for a second year in a row. Retrieved from https://www.nytimes.com/2025/06/24/nyregion/nyc-heat-wave.html

Hoyer, S., & Hamman, J. (2017). Xarray: N-D labeled arrays and datasets in Python. *Journal of Open Research Software*, *5*(1), 10. https://doi.org/10.5334/jors.148

Hunter, J. D. (2007). Matplotlib: A 2D graphics environment. *Computing in Science & Engineering*, *9*(3), 90–95. https://doi.org/10.1109/MCSE.2007.55

Ivanovich, C. (2026). ccivanovich/Extreme_Heat_Seasonality: AGU advances submission [Software]. *Zenodo*. https://doi.org/10.5281/zenodo.19582097

Ivanovich, C. C., Cook, B. I., & McDermid, S. (2026). Dry versus humid heat seasonality and drivers in the north American monsoon Region. *Journal of Geophysical Research: Atmospheres*, *131*(11), e2025JD045713. https://doi.org/10.1029/2025JD045713

Ivanovich, C. C., Sobel, A. H., Horton, R. M., Nunes, A. M. B., Da Rocha, R. P., & Camargo, S. J. (2025). Physical drivers of the November 2023 heatwave in Rio de Janeiro. *Weather and Climate Dynamics*, *6*(4), 1857–1874. https://doi.org/10.5194/wcd-6-1857-2025

Ivanovich, C. C., Sobel, A. H., Horton, R. M., & Raymond, C. (2024). Stickiness: A new variable to characterize the temperature and humidity contributions toward humid heat. *Journal of the Atmospheric Sciences*, *81*(5), 819–837. https://doi.org/10.1175/JAS-D-23-0072.1

Jacobson, T. W. P., Seager, R., Williams, A. P., Simpson, I. R., McKinnon, K. A., & Liu, H. (2024). An unexpected decline in spring atmospheric humidity in the interior southwestern United States and implications for forest fires. *Journal of Hydrometeorology*, *25*(3), 373–390. https://doi.org/10.1175/JHM-D-23-0121.1

Jha, R., Perkins-Kirkpatrick, S. E., Singh, D., Kimutai, J., Libonati, R., & Mondal, A. (2025). Extreme terrestrial heat in 2024. *Nature Reviews Earth & Environment*, *6*(4), 234–236. https://doi.org/10.1038/s43017-025-00661-2

Jones-Ngo, C. G., Ludwick, S., Al-Hamdan, M. Z., Vargo, J., Schmidt, R. J., Monier, E., & Conlon, K. C. (2025). Increasing exposures to compound wildfire smoke and extreme heat hazards in California, 2011–2020. *Earth's Future*, *13*(6), e2024EF005189. https://doi.org/10.1029/2024EF005189

Körner, C., Möhl, P., & Hiltbrunner, E. (2023). Four ways to define the growing season. *Ecology Letters*, *26*(8), 1277–1292. https://doi.org/10.1111/ele.14260

Lee, M., Nordio, F., Zanobetti, A., Kinney, P., Vautard, R., & Schwartz, J. (2014). Acclimatization across space and time in the effects of temperature on mortality: A time series analysis. *Environmental Health*, *13*(1), 89. https://doi.org/10.1186/1476-069X-13-89

Lemus-Canovas, M., Insua-Costa, D., Trigo, R. M., & Miralles, D. G. (2024). Record-shattering 2023 spring heatwave in western Mediterranean amplified by long-term drought. *npj Climate and Atmospheric Science*, *7*(1), 25. https://doi.org/10.1038/s41612-024-00569-6

Lewis, S. C., & King, A. D. (2017). Evolution of mean, variance and extremes in 21st century temperatures. *Weather and Climate Extremes*, *15*, 1–10. https://doi.org/10.1016/j.wace.2016.11.002

Lin, W., & Wang, C. (2022). Longer summers in the Northern Hemisphere under global warming. *Climate Dynamics*, *58*(9–10), 2293–2307. https://doi.org/10.1007/s00382-021-06009-y

Marengo, J. A., Costa, M. C., Cunha, A. P., Espinoza, J.-C., Jimenez, J. C., Libonati, R., et al. (2025). Climatological patterns of heatwaves during winter and spring 2023 and trends for the period 1979–2023 in central South America. *Frontiers in Climate*, *7*, 1529082. https://doi.org/10.3389/fclim.2025.1529082

Matthews, T., Raymond, C., Foster, J., Baldwin, J. W., Ivanovich, C., Kong, Q., et al. (2025). Mortality impacts of the most extreme heat events. *Nature Reviews Earth & Environment*, *6*(3), 193–210. https://doi.org/10.1038/s43017-024-00635-w

Matthews, T., Wilby, R. L., & Murphy, C. (2019). An emerging tropical cyclone–deadly heat compound hazard. *Nature Climate Change*, *9*(8), 602–606. https://doi.org/10.1038/s41558-019-0525-6

Milrad, S. M., Ennis, K. E., Knight, D. A., Dello, K. D., Raye, L., & Wodzicki, K. R. (2025). Cruel summer (and autumn): Humid heat trends, extremes, and mechanisms in the Southeast United States. *International Journal of Climatology*, *45*(8), e8837. https://doi.org/10.1002/joc.8837

Mora, C., Dousset, B., Caldwell, I. R., Powell, F. E., Geronimo, R. C., Bielecki, C. R., et al. (2017). Global risk of deadly heat. *Nature Climate Change*, *7*(7), 501–506. https://doi.org/10.1038/nclimate3322

NYC Public Schools. (2026). Sustainability. Retrieved from https://www.schools.nyc.gov/school-life/space-and-facilities/sustainability

Orlowsky, B., & Seneviratne, S. I. (2012). Global changes in extreme events: Regional and seasonal dimension. *Climatic Change*, *110*(3–4), 669–696. https://doi.org/10.1007/s10584-011-0122-9

OSHA Technical Manual. (2017). U.S. Department of Labor, occupational safety and health administration. Retrieved from https://www.osha.gov/otm/

Pampuch, L. A., Bueno, P. G., Reboita, M. S., Tomaziello, A. C. N., Nunes, A. M. P., Cardoso, A. A., et al. (2025). Brazil climate highlights 2023. *Annals of the New York Academy of Sciences*, *1549*(1), 120–138. https://doi.org/10.1111/nyas.15394

Park, B.-J., Kim, Y.-H., Min, S.-K., & Lim, E.-P. (2018). Anthropogenic and natural contributions to the lengthening of the summer season in the Northern hemisphere. *Journal of Climate*, *31*(17), 6803–6819. https://doi.org/10.1175/JCLI-D-17-0643.1

Parker, L. E., McElrone, A. J., Ostoja, S. M., & Forrestel, E. J. (2020). Extreme heat effects on perennial crops and strategies for sustaining future production. *Plant Science*, *295*, 110397. https://doi.org/10.1016/j.plantsci.2019.110397

Parsons, K. (2006). Heat stress standard ISO 7243 and its global application. *Industrial Health*, *44*(3), 368–379. https://doi.org/10.2486/indhealth.44.368

Perkins-Kirkpatrick, S., Barriopedro, D., Jha, R., Wang, L., Mondal, A., Libonati, R., & Kornhuber, K. (2024). Extreme terrestrial heat in 2023. *Nature Reviews Earth & Environment*, *5*(4), 244–246. https://doi.org/10.1038/s43017-024-00536-y

Raymond, C., Matthews, T., & Horton, R. M. (2020). The emergence of heat and humidity too severe for human tolerance. *Science Advances*, *6*(19), eaaw1838. https://doi.org/10.1126/sciadv.aaw1838

Raymond, C., Shreevastava, A., Slinskey, E., & Waliser, D. (2024). Linkages between atmospheric rivers and humid heat across the United States. *Natural Hazards and Earth System Sciences*, *24*(3), 791–801. https://doi.org/10.5194/nhess-24-791-2024

Rogers, C. D. W., Ting, M., Li, C., Kornhuber, K., Coffel, E. D., Horton, R. M., et al. (2021). Recent increases in exposure to extreme humid-heat events disproportionately affect populated regions. *Geophysical Research Letters*, *48*(19), e2021GL094183. https://doi.org/10.1029/2021GL094183

Rubio, M., Batchelor, M., & Gettel, A. (2025). *2024 heat-related deaths report* (p. 24). Maricopa County Department of Public Health. Retrieved from https://www.maricopa.gov/ArchiveCenter/ViewFile/Item/5934

Sambou, M. G., Pohl, B., Janicot, S., Landry Famien, A. M., Roucou, P., Badiane, D., & Gaye, A. T. (2021). Heat waves in spring from Senegal to Sahel: Evolution under climate change. *International Journal of Climatology*, *41*(14), 6238–6253. https://doi.org/10.1002/joc.7176

Sanap, S. D., Priya, P., Chowdary, J. S., Pattanaik, D. R., Jenamani, R. K., Rai, R., & Kumar, V. (2025). On the contrasting springtime extremes in India: Heatwaves and hailstorms in 2022 and 2023. *Quarterly Journal of the Royal Meteorological Society*, *152*(774), e70022. https://doi.org/10.1002/qj.70022

Schauberger, B., Archontoulis, S., Arneth, A., Balkovic, J., Ciais, P., Deryng, D., et al. (2017). Consistent negative response of US crops to high temperatures in observations and crop models. *Nature Communications*, *8*(1), 13931. https://doi.org/10.1038/ncomms13931

Schwarz, L., Malig, B., Guzman-Morales, J., Guirguis, K., Ilango, S. D., Sheridan, P., et al. (2020). The health burden of fall, winter and spring extreme heat events in Southern California and contribution of Santa Ana Winds. *Environmental Research Letters*, *15*(5), 054017. https://doi.org/10.1088/1748-9326/ab7f0e

Scott, T. J., White, R. H., & Donner, S. D. (2026). Summers over land and ocean are becoming longer, transitioning faster, and accumulating more heat. *Environmental Research Letters*, *21*(7), 074009. https://doi.org/10.1088/1748-9326/ae5724

Singh, D., McDermid, S. P., Cook, B. I., Puma, M. J., Nazarenko, L., & Kelley, M. (2018). Distinct influences of land cover and land management on seasonal climate. *Journal of Geophysical Research: Atmospheres*, *123*(21). https://doi.org/10.1029/2018JD028874

Sulikowska, A., & Wypych, A. (2021). Seasonal variability of trends in regional hot and warm temperature extremes in Europe. *Atmosphere*, *12*(5), 612. https://doi.org/10.3390/atmos12050612

Ting, M., Lesk, C., Liu, C., Li, C., Horton, R. M., Coffel, E. D., et al. (2023). Contrasting impacts of dry versus humid heat on US corn and soybean yields. *Scientific Reports*, *13*(1), 710. https://doi.org/10.1038/s41598-023-27931-7

Van Loon, A. F., Tijdeman, E., Wanders, N., Van Lanen, H. A. J., Teuling, A. J., & Uijlenhoet, R. (2014). How climate seasonality modifies drought duration and deficit. *Journal of Geophysical Research: Atmospheres*, *119*(8), 4640–4656. https://doi.org/10.1002/2013JD020383

Virtanen, P., Gommers, R., Oliphant, T. E., Haberland, M., Reddy, T., Cournapeau, D., et al. (2020). SciPy 1.0: Fundamental algorithms for scientific computing in Python. *Nature Methods*, *17*(3), 261–272. https://doi.org/10.1038/s41592-019-0686-2

Wang, J., Guan, Y., Wu, L., Guan, X., Cai, W., Huang, J., et al. (2021). Changing lengths of the four seasons by global warming. *Geophysical Research Letters*, *48*(6), e2020GL091753. https://doi.org/10.1029/2020GL091753

Weller, E., Park, B.-J., & Min, S.-K. (2020). Anthropogenic and natural contributions to the lengthening of the Southern hemisphere summer season. *Journal of Climate*, *33*(24), 10539–10553. https://doi.org/10.1175/JCLI-D-20-0084.1

Wu, S., Luo, M., Wang, X., Ge, E., Zhang, W., Gu, X., & Liu, J. (2023). Season-dependent heatwave mechanisms: A study of southern China. *Weather and Climate Extremes*, *42*, 100603. https://doi.org/10.1016/j.wace.2023.100603

Xu, Z., Cheng, J., Hu, W., & Tong, S. (2018). Heatwave and health events: A systematic evaluation of different temperature indicators, heatwave intensities and durations. *Science of the Total Environment*, *630*, 679–689. https://doi.org/10.1016/j.scitotenv.2018.02.268

Xu, Z., FitzGerald, G., Guo, Y., Jalaludin, B., & Tong, S. (2016). Impact of heatwave on mortality under different heatwave definitions: A systematic review and meta-analysis. *Environment International*, *89*(90), 193–203. https://doi.org/10.1016/j.envint.2016.02.007

Zachariah, M., Arulalan, T., AchutaRao, K., Saeed, F., Jha, R., Dhasmana, M. K., et al. (2023). Attribution of 2022 early-spring heatwave in India and Pakistan to climate change: Lessons in assessing vulnerability and preparedness in reducing impacts. *Environmental Research: Climate*, *2*(4), 045005. https://doi.org/10.1088/2752-5295/acf4b6

Zscheischler, J., Westra, S., van den Hurk, B. J. J. M., Seneviratne, S. I., Ward, P. J., Pitman, A., et al. (2018). Future climate risk from compound events. *Nature Climate Change*, *8*(6), 469–477. https://doi.org/10.1038/s41558-018-0156-3